Hole Configuration Effect on Turbine Blade Cooling

A.Hasanpour, M. Farhadi and H.R. Ashorynejad

Abstract—In this paper a numerical technique is used to predict the metal temperature of a gas turbine vane. The Rising combustor exit temperatures in gas turbine engines necessitate active cooling for the downstream turbine section to avoid thermal failure. This study is performed the solution of external flow, internal convection, and conduction within the metal vane. Also the trade-off between the cooling performances in four different hole shapes and configurations is performed. At first one of the commonly used cooling hole geometry is investigated; cylindrical holes and then two other configurations are simulated. The average temperature magnitude in mid-plan section of each configuration is obtained and finally the lower temperature value is selected such as best arrangement.

Keywords—Forced Convection, Gas Turbine Blade, Hole Configuration

I. INTRODUCTION

IMPROVING the performance of gas turbines can be achieved by increasing the turbine inlet temperature. This subject requires highly effective cooling techniques to maintain the temperature of the components in contact with the hot gases at acceptable levels. Film-cooling has been widely used to protect gas turbine blades from hot gases by injecting compressor bleed air through discrete holes in the blade surface [1-3]. Protecting the blade surface by means of film-cooling is tested by reducing the adiabatic wall temperature. Sieverding and Wilputte [7], Friedrichs et al [8] Kost and Nicklas [9], and Barigozzi et al [10] have reported aerodynamic benefits associated with end wall film-cooling in the form of reduction of the size and strength of the passage vortex and a reduction in strength of the cross passage flow.

However, there is an aerodynamic downside to film-cooling injection, as Friedrichs et al [11] reported that film-cooling ultimately increases the total pressure losses through the passage. They showed that the additional losses generated within the hole and the losses generated by coolant mixing with the free stream outweigh the reduction in losses associated with a reduction in secondary flows.

A study comparing total pressure losses between an uncooled endwall, a cooled endwall with cylindrical holes, and a cooled endwall with shaped holes was performed by Barigozzi et al [10]. They reported that there was no significant difference between the secondary flow fields with cylindrical holes versus conical diffuser shaped holes. They showed that for low injection rates, the magnitude of the total pressure losses in the loss core of the passage vortex increased relative to the uncooled case. Barigozzi et al[10] storied almost the same performance in terms of film-cooling effectiveness for the two different hole shapes at low mass flow rates, but reported significantly better cooling performance by the shaped holes at high mass flow rates. Note that their investigation featured diverse hole patterns in each passage, which meant that it was not a direct one-to-one comparison. Colban et al [12] compared the film-cooling performance of cylindrical holes and fan-shaped holes on a turbine vane endwall. They had the same experimental setup as the current study, with two passages having the same layout, one with cylindrical holes and the other with fan-shaped holes. The missing element in the research that has been performed is the investigation into the effect of difference holes configuration and shape on the cooling the gas turbine vane and comparing the result in clear parameters.

II. NUMERICAL SIMULATION

A. Model Geometry

At first it has been modeled case 1(Fig.1) for validation. Then other cases (2-4) are simulated and then compare them with two parameters. One of them is steadying the temperature profile on the blade surface and the other is decreasing average temperature on the blade. When these traits are satisfied the failure possibility of gas turbine vane that happened because of thermal gradient and thermal stresses is going to be les and les. The experimental data for validation of the this study for case 1, need to provide clear boundary conditions and cooling air flow rates of high accuracy. The C3X transonic-turbine guide vane of Hylton et al [13] was selected as the test case, for this work provides detailed measurement of the external and internal convection and the metal surface temperature. The experimental facility consisted of a linear cascade of three C3X turbine vanes. The center vane was cooled by air flowing through ten round flow passages from the hub to the shroud.

A. Hasanpour is MSc student at Faculty of Mechanical Engineering in the Babol University of Technology, Babol, P. O. Bax 484, I. R. Iran (E-mail: arman.hasanpour.87 @gmail.com).

M. Farhadi is assistant professor of Mechanical Engineering Department in the Babol University of Technology, Babol, I. R. Iran. (Corresponding author to provide phone: +98-111-3234205; E-mail: mfarhadi@nit.ac. ir).

H. R. Ashorynejad is MSc student at Faculty of Mechanical Engineering in the the Noshirvani University of Technology, Babol, I. R. Iran (h.r.ashorynezhad@gmail.com)

Fig. 1 C3X Vane with Cooling Holes

In their studies the heat transfer measurements were obtained by measuring the internal and external boundary conditions of the test piece at thermal equilibrium and solving the steady-state heat conduction equation for the internal temperature field of the test piece [13]. Temperature distributions were directly obtained from the normal temperature gradient at the surface. The cooling holes are approximately centered on the curvature line of the vane, except for the two holes near the leading edge. The cross section of this vane is shown in Fig.1 with the placement and size of the cooling holes marked by white circles. Detailed geometric parameters are listed in Table 1.

TABLE I
GEOMETRY PARAMETERS FOR C3X VANE

Throat (mm)	32.9
Vane spacing (mm)	117.7
Suction surface arc (mm)	177.8
Pressure surface arc (mm)	137.2
chord (mm)	144.9

Once this topology was generated, it was a relatively straightforward process to produce a grid. The topology needed to be generated by hand, which turned out to be very time consuming for a complex geometry like that of C3X. Among the features that were desirable for viscous grids is that the grids are clustered along the solid boundaries. Grid generator, Gambit ^{TM} was used with the topology to generate the final grid.

B. Numerical Methodology

The present computations employed periodicity conditions to replicate the multiple vane passages in the experiment, and therefore only one vane was included in the domain. All other parameters were taken from the experiment set-up data. The inlet is located one chord length upstream of the leading edge, where the turbulence level was measured in the experiments. The outlet is located one chord length downstream of the trailing edge. Meshes are created for the hot gas path and the solid vane. The flow was assumed to be fully developed at the hole inlets at the hub of the vane, as there were long tubes feeding the channels in the experiment. The coolant exited the top of the vane to atmospheric pressure. The heat transfer coefficients for the internal flow in the cooling holes were obtained from the correlation [13, 14]:

$$Nu_D = C_r(0.022 \, \text{Pr}^{0.5} \, \text{Re}_D^{0.8}) \tag{1}$$

The constant Cr in Eq.1 accounts the thermal entrance effects for the cooling channels [13]. The hot gas flow path details and cooling channel geometries and the coolant conditions are specified in Table 2and Table 3 respectively. The vane material is ASTM type 310 stainless steel [15], which has the constant density (ρ) of 7900 kg/m3 and the specific heat (Cp) of 586.15 J/kg.K. The thermal conductivity is specified to vary linearly with temperature over the range (from York [16]) in the simulations, as given by:

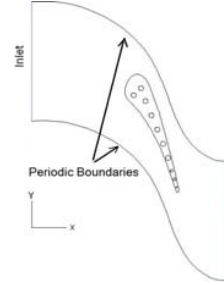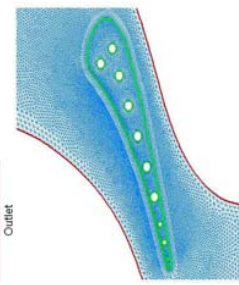$$k = 0.020176 \, T + 6.811 \, [\text{W/m-K}] \tag{2}$$

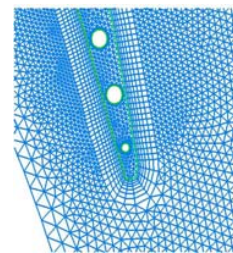

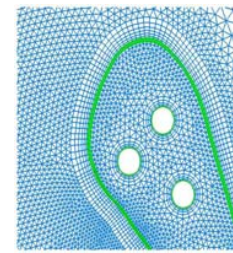Fig. 2 Computational Domain   Fig. 3 C3X Grid

Fig. 4 LE Enlargement   Fig. 5 - TE Enlargement

TABLE II
HOT GAS PATH FLOW DETAILS

Case	Ma (LE)	Ma (TE)	Re	T0 (K)	P0 (bar)
1	0.17	0.88	$1.9*10^6$	796	3.2

TABLE III
COOLING CHANNEL'S PROPERTY

N	1	2	3	4	5	6	7	8	9	10
T K)	387	388	371	376	355	412	367	356	406	420
φ(mm)	6.3	6.3	6.3	6.3	6.3	6.3	6.3	3.1	3.1	1.98

A super-block numerical grid was used in the present work to allow the highest quality in all regions with the fewest numbers of cells (40000 cells). A two-dimensional grid was first created in Gambit ^{TM} from FLUENT INC. The present simulations employed two variants of the popular, two-equation k-ε model for comparison purposes. The first model was the "standard" k-ε (S-kε) model originally proposed by Launder and Spalding [17]. The second model was a realizable k-ε (R- k-ε) turbulence model, which is documented by Shih et al. [18]. The R-kε model satisfies the so called realizability constraints for the Reynolds stresses, specifically requiring positivity of the Reynolds normal stresses and satisfaction of Schwarz's inequality for the shear stresses. This

model has been shown by several researchers to reduce the excessive and non-physical production of turbulent kinetic energy characteristic of the standard k-ε model in areas of high irrotational strain. This strain condition occurs at the stagnation point on the leading edge of a turbine airfoil and downstream of the leading edge on the suction side. Walters and Leylek [19] documented the superior performance of the R-kε model in a simulation of a turbine airfoil cascade. The two-layer near-wall model of Wolfstein [20] was employed to resolve the flow all the way to the wall, including the viscous sub-layer. The present simulations were run using the FLUENTTM 6.3.26 code from FLUENT INC., Inc. In the fluid zones, the steady, timed-averaged Navier-Stokes equations were solved, and pressure-velocity coupling was achieved with a pressure-correction algorithm. In the solid zone, the Fourier equation for heat diffusion was solved. All equations were discretized with second-order accuracy. At the fluid-solid interfaces, an energy balance was satisfied at each iteration, such that the heat flux at the wall on the fluid side was equal in magnitude and opposite sign to the heat flux on the solid side. The temperature of the boundary itself was adjusted during each iteration to meet this condition. Thus, all fluid-solid interfaces were fully coupled. A final solution was confirmed only after grid-independence was established. The hanging node adaption technique was employed to retain the high quality of the background grid. A converged solution was then obtained with the adapted grid.

C. Hole Configurations

Most often, the holes on the blade tip are arranged on the mid camber line of the tips due to manufacturing reasons. However, the simple camber line film-hole arrangement may not yield a good design for blade tip film cooling applications since the film cooling jets do not provide adequate coverage for the high heat transfer regions on either the plane or squealer blade tips. For the plane tip case, Kwak and Han [21, 22] observed than the high heat transfer region was located on the pressure side of the blade tip. By this reasons in this paper other configurations and arrangements of cooling holes were simulated. At first, for validation with experimental results (Hylton et all [13]), the conventional film cooling holes (Figs1-5) was modeled and then other well-known hole configurations were studied (Fig.6)([3] and [23]). After modeling the different hole shapes a comparison between each other of them are done. The compression parameters are steadying the temperature profile on the blade surface and decreasing average temperature. The first parameter can be judge by temperature couture and the second by the average temperature. By this comparisons between cases (2 and 3), the selection of best hole arrangements could be done.
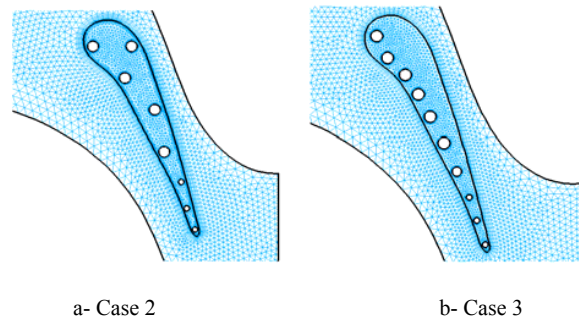

a- Case 2   b- Case 3

Fig. 6 Cases grid

III. RESULTS AND DISCUSSIONS

A. C3X Model

The result of the simulation are presented and analyzed in this section. Two simulations are discussed with different turbulence models, the S-k-ε and R-k-ε. At first the result for case1 (Figs.1-5) are shown (in Figs.7-12) and validate with experimental results [13].Then the temperature profiles for other configurations and arrangements (case 2, 3) (Fig.6) are presented (Fig.15). In Fig. (7) for suction side (-1≤x/s≤0), the pressure falls very rapidly from the stagnation line toward the throat, reaching a minimum value of static pressure by x/s = -0.25. A mild adverse pressure gradient follows this minimum, and after x/s = -0.5, a soft acceleration arises to the trailing edge. On the pressure side (0≤x/s≤1), the pressure stays almost constant near P0 from the LE to about x/s = 0.5 and then falls off with further distance toward the TE. The calculations reveal good agreement with the data of Hylton et al. [13],(Figs,7 and 8). Figure 8 shows the heat transfer coefficient normalized by h_{ref} (1135 w/m2.K) along the vane surface by Realizable k-ε (R-kε) and standard k-ε model (S-kε) and contrast with experimental data. Results generally are small percent higher compared to the experimental data. The difference between experimental and computational data near the leading edge can be because of acceleration after stagnation point and FULENT software cannot predict the behavior of flow at this point, thoroughly.
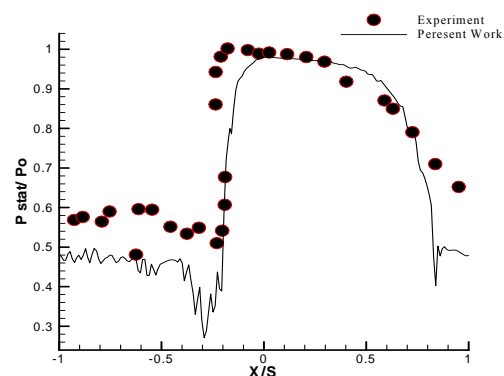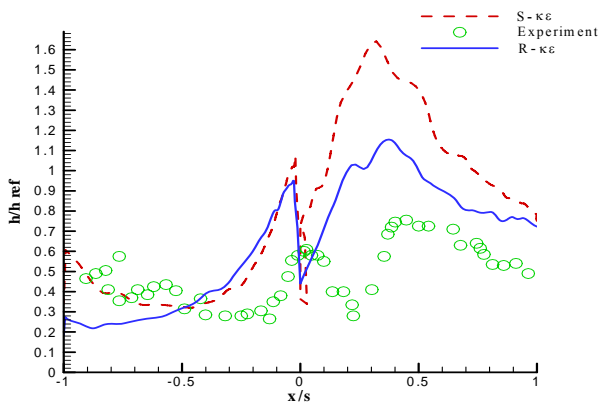

Fig.7 Experimental and calculated data of Pstat / P_0

Fig. 8 Experimental and calculated data of h / h$_{ref}$

From the results it can be seen that the enough pragmatic results are obtained by Realizable k-ε (R-kε) model. Therefore the R-kε result is plotted. The contour of Mach number on vane surface is shown in Figure 9. Due to the shape of the airfoil, the flow sees strong acceleration along the suction side near the leading edge. The maximum Mach number in the vane passage is about Ma=0.85 and it occurs at a position just off the SS about 20% of the distance from the LE to TE. The Mach number remains quite low near the pressure side until the aft quarter of the vane, when the flow accelerates to the TE mach number of about 0.8. Notice also that the maximum Mach numbers in some of the cooling channels exceed Ma=0.75, meaning the internal flow is also compressible.
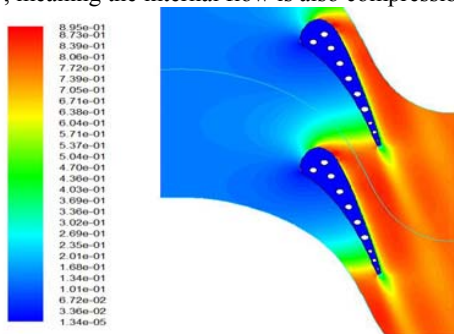

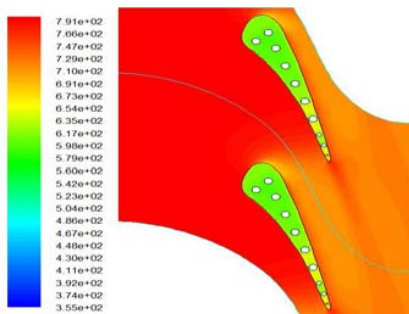Fig. 9 Contours of Mach number

Fig. 10 Contours of Static Temperature

The stream lines of hot gas flow on blade surface are shown in Figure 11. Figure 12 shows the stagnation point enlargement and stagnation point illustrated with bold point.

It is clear that mainstream near the stagnation point has dual actions. When the main flow across the vane, it had to be stopped. A part of this flow goes to the upper than stagnation point and makes the suction side and scantling stream of hot gas flow goes lower of this point and creates pressure side.
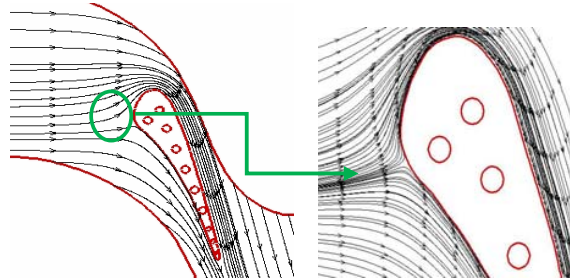

Fig. 11 Stream lines on the blade   Fig. 12 Stagnation point

B. Other Hole Configurations

In this section the result of other configurations and arrangements of cooling holes are indicated. Because of comparison the result, Fig.13 shown the temperature profiles for the case2 and 3 (Fig-6) and the magnitude of average temperature on the vane surfaces are listed in table 4.

TABLE IV
AVERAGE TEMPERATURE ON THE VANE SURFACE

Case	2	3
Average Static Temperature (K)	658	664

Fig. 13 exposes the temperature profiles of case 2, 3 and 4(Fig-6). It is clear that in the case 2 streaming of blade temperature are very steady. Perhaps it be seems that in another case this state had been happened. But by respect to the average temperature such as other parameter for comparison is considered (Table 4) it is clear that this parameter in case 4 is smaller than another configuration. By this reason case 2 is selected such as best arrangement and configuration between the hole shapes. It means that with this hole shapes the vane resistance can be improved in relation to thermal collapse and satisfied the blade cooling goal.
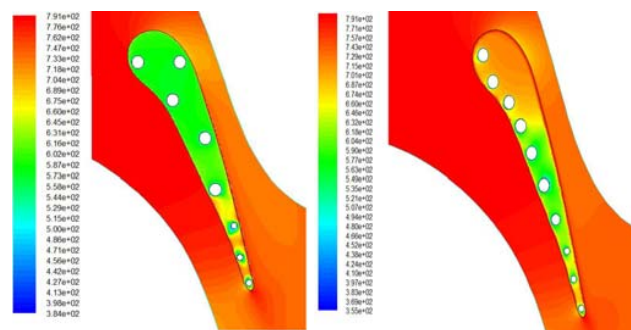
a- Case 2   b- Case 3

Fig. 13 Contours of Static Temperature

IV. CONCLUSION

A numerical methodology for conjugate heat transfer simulations has been applied. The present study was designed to high-light the promise of this relatively new tool in gas turbine heat transfer design, wherein the individual heat transfer problems (external/internal convection, conduction in the metal) are coupled in a single simulation. The benefits of the conjugate approach are inherently better accuracy and reduced turn-around time as compared to the common practice of decoupled simulations. The vane was cooled by air flowing radially through ten smooth-walled channels. The predicted mid-span temperature distribution on the vane external surface was in reasonable agreement with experimental data when the realizable k- ε (RKE) turbulence model was used. The standard k-ε model did not perform as well, and showed a positive offset in predicted temperature as compared to the RKE model and the experimental data. There is room for improvement in the turbulence modeling aspect of this methodology, such as the implementation of a model that can accurately predict boundary layer transition. With the methodology validated, the computational results were fully analyzed. The highest metal temperature and largest temperature gradients were located at the trailing edge of the vane where the metal is very thin. The metal temperature everywhere was much closer to the temperature in the passage free stream than the coolant temperature. This was due to the fact that the thermal resistance due to internal convection was much greater than the resistance of the external convection or the conduction within the metal.

REFERENCES

[1] B.Dennis, I.Egorov, G.Dulikravich, S.Yoshimura, Optimisation of a Large Number Coolant Passages Located Close to the Surface of a Turbine Blade, ASMEPaperGT2003-38051, 2003.

[2] Zhihong Gao, DigantaP.Narzary, Je-ChinHan,2008, Film cooling on a gas turbine blade pressure side or suction side with axial shaped holes, International Journal of Heat and Mass Transfer 51,2139–2152

[3] Grzegorz Nowak, Wlodzimierz Wroblewski, 2009, Cooling system optimization of turbine guide vane: 567–572, Applied Thermal Engineering 29

[4] Kercher, D.M., 2003. Film-cooling bibliography: 1940–2002, Private publication.

[5] Kercher, D.M., 2005. Film-cooling bibliography addendum: 1999–2004, Private publication

[6] Bogard, D.G., Thole, K.A., 2006. Gas turbine film cooling. AIAA J. Prop. Pow. 22, 249–270.

[7] Sieverding, C.H., Wilputte, P., 1981. Influence of mach number and endwall cooling on secondary flows in a straight nozzle cascade ASME J. Eng. Gas Turb. Pow. 103, 257–264.

[8] Friedrichs, S., Hodson, H.P., Dawes, W.N., 1995. Distribution of filmcooling effectiveness on a turbine endwall measured using the ammonia and diazo technique. ASME J. Turbo. 118, 613–621.

[9] Kost, F., Nicklas, M., 2001. Film-cooled turbine endwall in a transonic flow field: Part I – Aerodynamic measurements, ASME 2001-GT-0145.

[10] Barigozzi, G., Benzoni, G., Franchini, G., Perdichizzi, A., 2005. Fanshaped hole effects on the aero-thermal performance of a film cooled endwall, ASME GT2005-68544.

[11] Friedrichs, S., Hodson, H.P., Dawes, W.N., 1997. Aerodynamic aspects of endwall film-cooling. ASME J. Turbo. 119, 786–793.

[12] Colban, W., Thole, K.A., Haendler, M., 2006a. A comparison of cylindrical and fan-shaped film-cooling holes on a vane endwall at low and high freestream turbulence levels, ASME GT2006-90021.

[13] Hylton, Milhec, Turner, Nealy and York.(1983) "Analytical and Experimental Evaluation of the Heat Transfer Distribution Over the Surface of Turbine Vanes". NASA CR 168015.

[14] Jatin Gupta, B.Tech ,(2009,"Applicarion Of Conjugate Heat Transfer Methodology For Computation Of Heat Transfer On A Turbine Blade",), A Thesis Presented in Partial Fulfillment of the Requirements for the Degree Master of Science in the Graduate School of The Ohio State University

[15] Goldsmith, Waterman and Hirschhorn. (1961) "Handbook of Thermophysical Properties of Solid Materials - Volume II: Alloys". The Macmillan Company, New York, USA.

[16] York, D. W., and Leylek, J. H.,(2003),"Three-Dimensional Conjugate Heat Transfer Simulation of an Internally-Cooled Gas Turbine Vane", ASME Paper No. GT2003-38551,.

[17] Launder and Spalding. (1972) "Lectures in Mathematical Models of Turbulence". Academic Press, London, England.

[18] Shih, Liou, Shabbir and Zhu. (1995) "A New k-ε Eddy-Viscosity Model for High Reynolds

[19] Number Turbulent Flows: Model Development and Validation. Computers and Fluids". v. 24, no. 3, pp. 227-238.

[20] Walters and Leylek. (2000) "Impact of Film-Cooling Jets on Turbine Aerodynamic Losses". ASME Journal of Turbo-machinery, v.122, pp. 537-545.

[21] Wolfstein. (1969) "The Velocity and Temperature Distribution of One-Dimensional Flow With Turbulence Augmentation and Pres-sure Gradient," International Journal of Heat and Mass Transfer. v. 12, pp. 301-318.

[22] Kwak and Han. (2002) "Heat Transfer Coefficient and Film Cooling Effectiveness on a Gas

[23] Turbine Blade Tip". GT -2002-30194.

[24] Kwak and Han. (2002) "Heat Transfer Coefficient and Film Cooling Effectiveness on the

[25] Squealer Tip of A Gas Turbine Blade". GT-2002-30555.

[26] Uwe kruger ,karsten kusterer,Gernot Lang, Hauke Rosch, 2000,Analysis of the influence of cooling steam conditions on the cooling efficiency of a steam cooled vane using, conjugate calculation technique, Private publication-D-52070 Aachen-Germany, vol .5, pp.87-96.